Medio-lateral and lateral edge friction in indoor sports shoes

Bagehorn, Timo; Lysdal, Filip Gertz; Jakobsen, Lasse; de Zee, Mark; Kersting, Uwe Gustav

Published in:
Proceedings of the 13th annual meeting of the Danish Society of Biomechanics

Publication date:
2021

Document Version
Publisher's PDF, also known as Version of record

13th annual meeting of the Danish Society of Biomechanics

This year meeting will be hosted by Technical University of Denmark online using Zoom:

Join Zoom Meeting:

https://aaudk.zoom.us/j/63984164435

Meeting ID: 639 8416 4435

Passcode: DBS@DTU'21

Program:

10:00-10:10 Welcome by Lasse Jakobsen

10:10-10:50 **Keynote lecture**: Associate Professor Peter Johansen

Title: Experimental Cardiovascular Biomechanics

Chair: Marie Sand Traberg

11:00-12:00 Student competition (8 min + 2 min discussion)

1. **Presenter:** Hamed Shayestehpour
   Title: Musculoskeletal modeling of scoliosis patients with acceptable kinematic accuracy

2. **Presenter:** Bente Nielsen
   Title: HISTORY DEPENDENCE IN INDEX FINGER TAPPING

3. **Presenter:** Patrick Mai
   Title: MIMICKING GAME SCENARIOS IN A LABORATORY-BASED ENVIRONMENT: THE EFFECTS ON KNEE ABDUCTION MOMENT WHEN FACING VARIED TASK DEMANDS

4. **Presenter:** Gorm Henrik Fogh Rasmussen
   Title: Resistance training can induce hypoalgesia in women with persistent pain after breast cancer treatment

5. **Presenter:** Camilla Hoffmeyer Skadhauge
   Title: Test-Retest Reliability of a Novel Virtual Video Head Impulse Test

6. **Presenter:** Stefan Peter Engelmann Jensen
   Title: 3D KINEMATIC MODELLING OF SHOULDER BIOMECHANICS

Chair: Filip Gertz Lysdal

12:00-13:00 Lunch break

12:15-12:45 Generalforsamling Dansk Biomekanisk Selskab

13:10-14:00 Oral presentations (8 min + 2 min discussion)

7. **Presenter:** Cristina-Ioana Pirscoveanu
   Title: Does wearing a passive exoskeleton help during obstacle avoidance?

8. **Presenter:** Ernst Albin Hansen
   Title: FREELY CHOSEN CADENCE IS DEPENDENT ON PEDALLING HISTORY DURING ERGOMETER CYCLING

9. **Presenter:** Timo Bagehorn
   Title: MEDIO-LATERAL AND LATERAL EDGE FRICTION IN INDOOR SPORTS SHOES

10. **Presenter:** Ilias Theodorakos
    Title: Bone tracking using A-mode ultrasound probes: evaluation of the initial guess)

11. **Presenter:** Peter Christian Raffalt
    Title: The temporal pattern and the probability distribution of visual cueing can alter the structure of stride-to-stride variability)

Chair: Marie Sand Traberg

14:15-14:45 poster presentations (3 minutes + 3 min discussion)

12. **Presenter:** Kent Klitgaard
    Title: A Modified Single Arm Machine- A Brief Report

13. **Presenter:** Mohamed Amin Shayestehpour
    Title: The apical vertebrae in mild scoliotic spines are subject to minimum weight moments

14. **Presenter:** Mike Steffensen
    Title: TREND VALIDATION OF METABOLIC MODELS AGSINST MEASUREMENTS USING INDIRECT CALORIMETRY

15. **Presenter:** Cristina-Ioana Pirscoveanu
    Title: THE EFFECT OF MASS DISTRIBUTION OF A LOWER BODY PASSIVE EXOSKELETON ON JOINT MOMENTS

16. **Presenter:** Kevin Bill
    Title: THE EFFECT OF CUTTING TASK COMPLEXITY ON TECHNIQUE VARIABLES ASSOCIATED WITH INCREASED RISK OF ACL INJURIES IN FEMALE HANDBALL PLAYERS)

Chair: John Rasmussen

14:45-15:25 **Keynote lecture:** Professor Tron Krosshaug

Title: Biomechanics of cutting and landing – injury mechanisms and risk factors for ACL injury

Chair: Lasse Jakobsen

15:35-15:45 Announcement student award by Filip Gertz Lysdal

15:45-15:55 Announcement poster award by John Rasmussen

15:55-17:00 Closing – time for a cold one and networking.

DBS

Danish Society of Biomechanics

Sponsored by

DELSYS

EUROPE

Musculoskeletal modeling of scoliosis patients with acceptable kinematic accuracy

Hamed Shayestehpour[1,*], Mohammad Amin Shayestehpour[3], Christos Koutras[4], Christian Wong[2], and John Rasmussen[1]
[1]Department of Materials and Production, Aalborg University, Aalborg East, Denmark
[2]Department of Orthopedics, University Hospital of Hvidovre, Hvidovre, Denmark
[3]Department of Mechanical Engineering, Sharif University of Technology, Tehran, Iran
[4]Department of Computer Science, Rey Juan Carlos University, Madrid, Spain
Email: hs@mp.aau.dk

Introduction

The aetiology underlying **A**dolescent **I**diopathic **S**coliosis (AIS) has remained unclear [1]. An anatomically valid musculoskeletal model might contribute to uncovering the biomechanical cause. We previously developed and validated a spine model capable of simulating scoliosis deformities, with joint definition compatible with anatomical joint properties [2]. Further, we improved the muscle anatomy of the ribcage and the ribcage-scapula contact model [3].

In this study, we developed a semi-automated process to simulate scoliosis patients using all visible geometrical parameters retrieved from bi-planar radiographs, which improves the kinematics and, thus, the kinetic model.

Methods

In this study, we simulated 14 mild AIS cases with different lumbar, thoracolumbar, and thoracic curves. Firstly, the mannequin was scaled using the patient's height, mass, spine height, ribcage width, and depth. Secondly, we selected four corner nodes of all visible vertebrae in both sagittal and frontal X-rays, subsequently calculating the vertebrae's centers and angles. Further, the rib angles, C7 position relative to the sacrum, and rib humps were measured.

We utilized a least-squares optimization method in AnyBody Modeling System [4], which minimizes the kinematic error between the measured and model parameters. To investigate the accuracy of this method, we calculated the errors of some known clinical parameters, including lumbar and thoracic Cobb angles (CobbL, CobbT), thoracic kyphosis (TK), lumbar lordosis (LL), rib hump from 10^{th} to 5^{th} rib pairs (RH), C7 translation relative to the sacrum in anteroposterior and mediolateral direction (C7T), and all rib angles (RibA). Further, the thoracic and lumbar apical vertebrae of the patients and the model were assessed to be matched as part of spine reconstruction validation.

Results and Discussion

The average and maximum errors for angles were 1.9 and 4.3 degrees, and distances were around 1.3 and 3.7mm. Besides, the apical vertebrae of the model were 100% corresponded to the radiographs. Figure 1 represents the average error of the parameters and the projection of the model to the radiographs of a patient.

Axial rotation of the vertebrae is not measurable from the X-rays directly. However, the model creates relevant axial rotation based on the rib angles and rib hump inputs without violating the costovertebral joint definition.

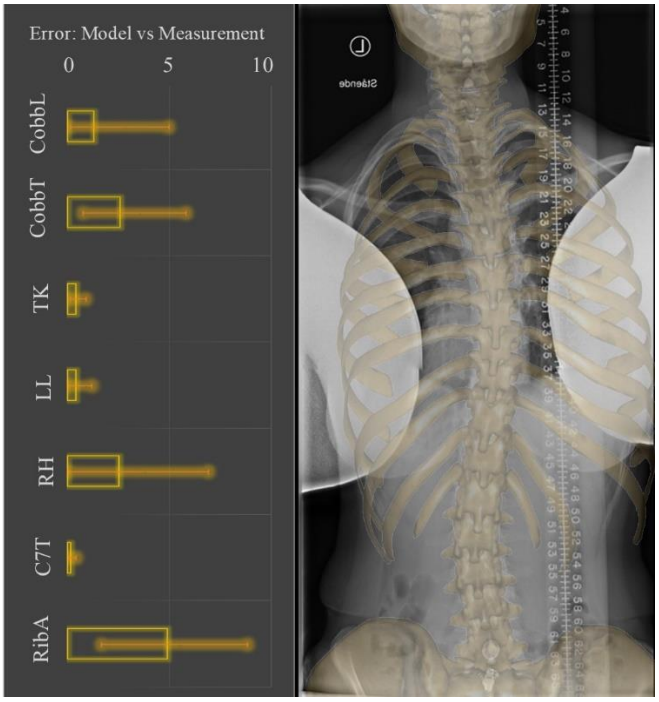

Figure 1: *Left:* The average error of the model together with the error bar of the parameters. The angle and distance errors are in degrees and mm, respectively. *Right:* The projection of the transparent model to the radiograph of a patient.

Conclusions

Since the acceptable measuring errors from radiographs are 5 degrees and 5 mm (or more), the model reconstructs the patients with an acceptable tolerance. Future use of the model will include investigating the pathomechanism behind AIS, simulation of brace effects, and optimization of brace treatments.

Acknowledgments

The project has received funding from the European Union's Horizon 2020 research and innovation programme under the Marie Sklodowska-Curie grant agreement NO. [764644].

References

[1] C. Wong, *Scoliosis*, 10-1, 1–5, 2015.
[2] H. Shayestehpour, et al., *Multibody Syst. Dyn.*, 2021.
[3] H. Shayestehpour, et al., *Journal of Biomechanics*,Submitted.
[4] M.S. Andersen, et al., *Computer Methods in Biomechanics and Biomedical Engineering*, 13-2, 171-183, 2010

HISTORY DEPENDENCE IN INDEX FINGER TAPPING

B. M. Nielsen[1,*], C. Fjordside[1,*], N. B. Jensen[*] & E. A. Hansen

Sport Sciences – Performance and Technology, Department of Health Science and Technology, Aalborg University, Denmark

[1]Shared first authorship. [*]Student.

INTRODUCTION

Finger tapping is a rhythmic, automated, stereotyped, motor task, which is widely performed in studies of motor control and behavior [1, 2]. History dependence can describe that motor output is dependent on previous activity. In the present study, it was investigated whether initial finger tapping at relatively low and high tapping rates would affect the subsequent freely chosen tapping rate at the end of the same bout of finger tapping.

METHODS

Healthy participants (10 males, 9 females: 1.75±0.11 m, 73.2±15.1 kg, 23.1±2.6 years) performed three different bouts, each consisting of 3 min of finger tapping. In the first bout (C), the tapping rate was freely chosen, throughout the bout. In another bout (A), the initial 50 s was performed at a volitional "markedly lower rate than the freely chosen finger tapping rate" for 50 s, which was followed by a freely chosen tapping rate for 2 min and 10 s. In yet another bout (B), the initial 50 s was performed at a volitional "markedly higher rate than the freely chosen finger tapping rate", which was followed by a freely chosen tapping rate for 2 min and 10 s. Bouts A and B were performed in counterbalanced order. The three bouts were separated by periods of two weeks [2, 3, 4, 5, 6]. The participants' tapping rate was determined in 15-s time periods, during the three bouts.

RESULTS

The data were not different from a normal distribution ($p>0.05$). At the end of tapping, the rate during bout A was 14.6±23.7% lower than during bout C ($p=0.023$).

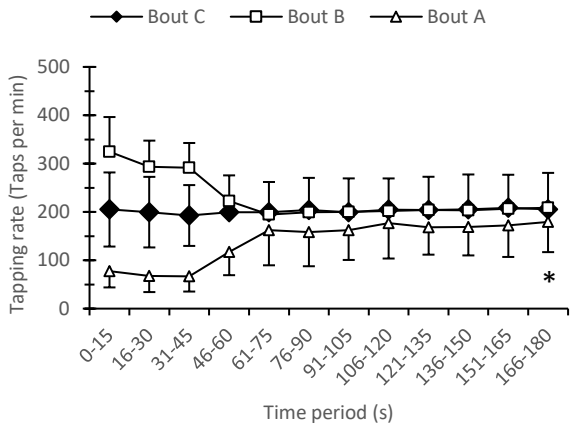

*Tapping rate as a function of time period during the three bouts. Data are mean±SD. SD-bars for bout A and B are only shown in one direction. SD-bars are only shown for the first three time periods, for bout C. All together, for clearness. *Different from bout C (p=0.023).*

DISCUSSION AND CONCLUSION

The freely chosen tapping rate is suggested to be generated by an interplay between supraspinal input, sensory feedback, and spinal neural networks (occasionally termed central pattern generators, CPGs) [2, 4, 5, 7].

The observed history dependence of the freely chosen tapping rate might be a result of neuromodulation caused by neurotransmitter substances [8].

Of interest, only the initial low tapping rate elicited history dependence. This might suggest that only inhibition occurred in the present study. It is unknown exactly where in the nervous system an inhibition could have occurred. Thus, it is unknown if it occurs on a spinal or on a supraspinal level [2, 4, 5, 7]. A combination could also have occurred.

Of note, history dependence of the freely chosen cadence during ergometer pedaling has been reported recently [9].

In conclusion, initial finger tapping at a relatively low preset target tapping rate caused the subsequent freely chosen tapping rate, at the end of the same bout of finger tapping, to be lower, as compared to a reference value of freely chosen tapping rate (at the end of bout C). The same was not observed when the initial tapping was performed at a relatively high preset target tapping rate.

REFERENCES

[1] Aoki T *et al*. (2005) Motor Control 9: 23-39
[2] Hansen EA *et al.* (2015) J Mot Behav 47: 490-496
[3] Hansen EA *et al.* (2020) J Mot Behav 52: 89-96
[4] Emanuelsen A *et al.* (2020) J Mot Behav 53:351-363
[5] Hansen EA & Ohnstad AE (2008) Exp Brain Res 186: 365-373
[6] Sardroodian M *et al.* (2015) J Mot Behav 48: 256-263
[7] Bucher D *et al.* (2015) In book: eLS, John Wiley & Sons 1-12
[8] Schibye B (2018) *Menneskets Fysiologi,* FADL'S forlag
[9] Hansen EA *et al*. (2021) Eur J Appl Physiol, Online ahead of print

ACKNOWLEDGEMENTS

Participants are thanked for their effort. Mikkel Ekknud Pedersen, AAU student, is thanked for his contribution to the work.

MIMICKING GAME SCENARIOS IN A LABORATORY-BASED ENVIRONMENT: THE EFFECTS ON KNEE ABDUCTION MOMENT WHEN FACING VARIED TASK DEMANDS

Patrick Mai[1,*], Kevin Bill[1,*], Katharina Glöckler[1,*], Mireia Claramunt-Molet[2,3,*], Julia Bartsch[5], Mathias Eggerud[5], Anniken Pedersen[4], Fredrik Sæland[5,*], Reidar Bergh Moss[4], Steffen Willwacher[6], Uwe Kersting[1], Ola Eriksrud[4] &Tron Krosshaug[5]
[1]Institute of Biomechanics and Orthopaedics, German Sport University, [2]Digital Health Unit, Eurecat Centre Tecnològic de Catalunya,[3]Biomechanical Engineering Lab, Universitat Politècnica de Catalunya, [4]Physical Performance, Norwegian School of Sports Sciences, [5]Sports Medicine, Norwegian School of Sports Sciences, [6]Mechanical and Process Engineering, Offenburg University; e-mail: p.mai@dshs-koeln.de, *Ph.D. student

INTRODUCTION

A high number of non-contact anterior cruciate ligament (ACL) injuries occur during cutting maneuvers [1]. The peak knee abduction moment (KAM) within the early phase of stance is a strong predictor of ACL injuries. Still, measuring knee joint loading in-field is challenging. However, to understand ACL loading, quantify the effectiveness of prevention programs, and to screen athletes, it may be necessary to mimic game-like scenarios in a controlled laboratory-based environment. Therefore, the purpose of this study was to compare KAM magnitudes and ranking consistency when simulating key game elements (catching a ball, faking defenders).

METHODS

Fifty-one female (mean±SD: 66.9±7.8 kg, 1.74±0.06 m, 19.2± 3.4 yrs) handball players volunteered. We captured the kinematics and kinetics of the full body with a marker-based tracking system (24 cameras, Qualisys AB, 200 Hz) and force plates (AMTI, 1000 Hz) during three standardized cutting tasks. For Task 1, athletes were instructed to perform a sidestep cut without catching a ball or faking a defender. For Task 2, athletes performed a sidestep cut after catching a ball to fake one static defender [2]. For Task 3, athletes were instructed to fake three dynamic opponents with a sidestep cut after catching a ball. Depending on the athlete's playing position, at least five cuts (per task) were collected on the dominantly exposed leg. The order of the tasks was randomized. Marker trajectories and force plate data were used to calculate joint kinematics and kinetics using a rigid body model with fore-, rearfoot, shank, thigh, and pelvis [3]. KAM within the first 100 ms of stance was identified and normalized to body mass. We applied a repeated-measures ANOVA ($\alpha<0.05$) to reveal the difference in the KAM between the three tasks. Post-hoc ($p_{posthoc}$) analysis was performed using Bonferroni corrections. Effect size was calculated using partial eta squared. To quantify if the ranking of the KAM changes across the three tasks, we calculated Spearman's rank correlation coefficient (r_s).

RESULTS AND DISCUSSION

The repeated-measures ANOVA revealed a statistically significant (p=0.02) task effect on the KAM (Figure 1). The KAM increased significantly ($p_{posthoc}$=0.012) from task 1 (1.57±0.29 Nm/kg) to task 2 (1.76±0.61 Nm/kg). A further significant ($p_{posthoc}<0.001$) increase when comparing task 1 to task 3 (1.85±0.25 Nm/kg) could be identified. When comparing task 2 to task 3, there was a 5% increase in the KAM on average. However, no significant difference was observed. When comparing the ranking of the KAM across the three tasks, we found a statistically significant relationship (Table 1). A very strong relationship (r_s=0.808) could be observed when comparing task 1 to task 3. Strong (r_s=0.622) and moderate (r_s=0.584) correlations were observed when comparing the ranking between task 2 vs. 3 and task 1 vs. 2, respectively.

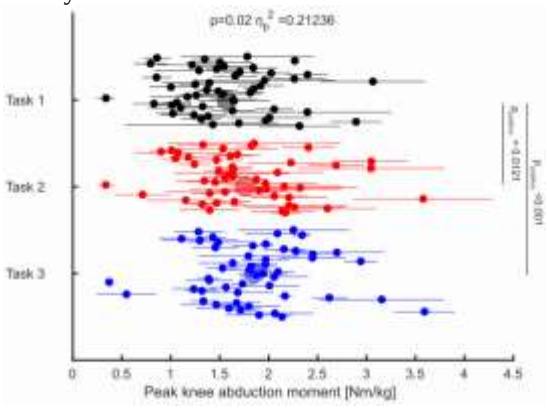

Fig. 1 Peak knee abduction moment for the three tasks. SD (error bars) of the five trials presents individual data.

CONCLUSIONS

The selection of tasks mimicking game-like situations in laboratory studies affects magnitudes of ACL-related loading parameters, while correlations of parameters between tasks are partly only moderate. Therefore, caution needs to be applied when assessing individual risks based on one single task. A simple pre-planned cut provides similar results as the complex, unanticipated cut (task 3). These results disregard the influence of neuromuscular control strategies which have been identified as important factors in previous work.

REFERENCES

1. Krosshaug T, et al., *Am J Sports Med*, **32**: 359-367, 2007
2. Kristianslund E, et al., *Br J Sports Med*, **48**: 779-783, 2014
3. Willwacher S, et al., *Footwear Sci*, **8**: 99-108, 2016

	Task 1 vs. Task 2	Task 1 vs. Task 3	Task 2 vs. Task 3
r_s	0.584	0.808	0.622
p	p<0.001	p<0.001	p<0.001

Table 1 Spearman's rank correlation coefficient and p-values. For each possible combination.

Resistance training can induce hypoalgesia in women with persistent pain after breast cancer treatment

G. H. F. Rasmussen[1]*, P. Madeleine[1], M. Arroyo-Morales[2], M. Voigt[1], M. Kristiansen[1].
[1]Sport Sciences - Performance and Technology, Department of Health Science and Technology, Aalborg University, 9220 Aalborg, Denmark.
[2]Department of Physical Therapy, Faculty of Health Sciences, Sport and Health Institute Research (IMUDS). Biohealth Institute Research Granada (IBS.Granada)
*Ph.D.-student

INTRODUCTION

Persistent pain in and around the surgical area affects 25-60% of patients who have received treatment for breast cancer (1). Resistance training (RT) is an effective non-pharmalogical approach to managing a variety of adverse effects to breast cancer treatment (2). Unfortunately, little is known of potential pain-relieving benefits of this training modality in a breast cancer population. RT has been shown to induce a transient reduction in sensitivity to noxious stimuli known as exercise induced hypoalgesia (EIH) in pain free and chronic pain populations (3). However, the possible EIH response to a single bout of RT in breast cancer survivors with persistent pain has yet to be determined. Therefore, the aim of this study was to examine the effect of a single bout of RT on mechanical pain sensitivity in women with persistent pain after breast cancer treatment.

METHODS

Twenty breast cancer survivors were recruited, with self-reported pain ≥ 3 on a 0-10 numeric rating scale after standard treatment. Each participant visited the lab on three occasion: 1) Familiarization 2) Normalization and 3) Investigation. In the normalization session, one repetition maximum (1RM) were assessed in each of the following exercises in chronological order; 1) Box squat, bench press, trapbar deadlift, bench pull and lat pulldown. In the investigation session, 3 sets of 10 repetitions at 60% of the established 1RM were performed for each exercise with 3-minute rest periods in between sets. Pressure pain thresholds (PPTs) were collected Pre and Post training over 17 locations distributed across the dorsal- and ventral shoulder regions of the affected side. Each location was measured twice, and a third time if the coefficient of variation was ≥ 20%. Movement-evoked pain (MEP) were assessed on a 0-10 numeric rating scale (0 = No pain, 10 = maximum pain) immediately following each set.

RESULTS AND DISCUSSION

PPTs of the ventral shoulder region increased following a single bout of submaximal RT (P = 0.039), indicating a localized reduction in pain sensitivity for this area (Fig 1). In contrast, there were no apparent change in PPTs located on the dorsal shoulder region (P = 0.838). There were no significant differences in MEP between exercises (P = 0.563), indicating that MEP was not affected by exercise order (Table 1).

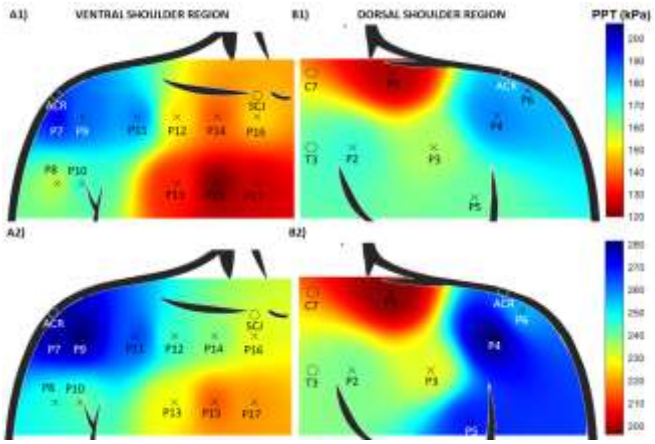

Fig. 1 Mean pressure pain threshold (PPT) maps for all anatomical locations pre (A1 & B1) and post (A2 & B2) a single bout of submaximal full body resistance training. Abbreviations; C7: Seventh cervical vertebrae, T3: Third thoracic vertebrae, ACR: acromion, SCJ: sternoclavicular joint.

CONCLUSIONS

Biomechanical loading of the shoulder girdle at 60% of 1RM adds to our knowledge about the sensory-motor interaction in breast cancer survivors. Actually, a single bout of submaximal RT reduces PPTs for the ventral shoulder region of breast cancer survivors with persistent pain after treatment. Accordingly, submaximal RT can be performed without concomitant short-term exacerbation of MEP, providing further support for RT as a safe and effective training modality for breast cancer survivors.

REFERENCES

1. Andersen KG et al., J Pain, 2011.
2. Santos W et al., BioMed Research, 2017.
3. Rice D et al., J Pain, 2019.

TABLE 1: Submaximal session loads & movement-evoked pain

EXERCISE	LOAD (KG)	MEP (0-10)
90º Box squat	29.8 (25.7:33.9)	1.0 (0.3:1.7)
Bench press	13.6 (12.1:15.0)	1.6 (0.7:2.5)
Trapbar deadlift	36.5 (33.0:39.9)	0.7 (0.1:1.3)
Bench press	17.8 (16.1:19.6)	1.1 (0.5:1.7)
Lat pulldown	19.0 (17.6:20.3)	1.1 (0.4:1.8)

Abbreviations: Movement-evoked pain, MEP.

Test-Retest Reliability of a Novel Virtual Video Head Impulse Test

Camilla H. Skadhauge[1*], Emma Hertel[1*], Nadja S. Kristensen[1*], Sissel H. Kronborg[1*] Dan D. Hougaard[2], and Afshin Samani[1]

[1]Department of Health Since and Technology, Sport sciences-performance and technology, Aalborg University, [2] Department of Otolaryngology, Head & Neck Surgery and Audiology, Aalborg University Hospital, Aalborg, Denmark

*Student

INTRODUCTION

Dizziness within the general population has a prevalence of 6.5% and is a common symptom in an array of diseases including vestibular disorders and stroke [1]. The numerous aetiologies presenting with similar symptoms elucidate why a quick and reliable diagnostic method is crucial to plan the treatment [2]. Currently, passive video head impulse testing can be used to achieve this by assessing the function of the six semi-circular canals within the inner ear by means of testing the vestibulo-ocular reflex (VOR) [3]. However, this method is not a "plug and play" examination as it requires highly trained personnel in order to conduct high-quality head impulses that are fast, abrupt, unpredictable, of high velocity, and with low amplitude [3]. Active head impulses can be utilized to circumvent this issue and to aid the general practitioner to diagnose more accurately. Though, the caveat is the anticipatory responses accompanying active movements may compensate for deficits of the VOR, thus, making the diagnosis difficult [4]. The field of virtual reality offers new possibilities for active head impulse testing with an adaptive environment which can be used to direct the active movements. Therefore, we propose a novel method for VOR testing combining traditional video-head impulse testing performed in a virtual reality environment.

METHODS

An experimental test-retest study of a head-mounted display with eye-tracking (HTC Vive, 120Hz; Pupil labs 120Hz binocular eye-tracking add-on for HTC Vive) for testing of the VOR was conducted on 12 healthy participants. Equipment was calibrated for each individual participant, ensuring high accuracy and precision. Passive head impulse testing was conducted by the investigator, while the participant fixated their gaze on a central fixation point. Active head impulses were self-generated head movements, directed by either visual or auditory commands. All head impulses were conducted in both the horizontal and vertical planes. Velocities, amplitudes, and peak accelerations were captured for both the head- and eye movements. VOR gain was calculated and defined as the ratio of the eye displacement and the head displacement. Moreover, cybersickness was assessed before and after exposure to virtual reality.

RESULTS AND DISCUSSION

All tests were found sufficient to produce normal VOR responses. VOR gains ranged from 0.77 to 0.84 in the active tests and from 0.80 to 0.93 in the passive tests, see figure 1. Excellent to good test-retest reliability was found for the passive tests, and moderate to poor reliability was found for the active tests [5]. Accuracy (range 3.17°-4.11°) and precision (range 0.61°-0.70°) were found to be lower when compared to previous reports [6]. A statistically significant increase in simulations sickness scores was observed, however, this increase was not categorized as clinically significant [7].

	VOR GAIN	
	SESSION 1 Mean (±SD)	SESSION 2 Mean (±SD)
PASSIVE HEAD IMPULSE TESTS		
Horizontal	0.93 (0.17)	0.93 (0.19)
Vertical	0.80 (0.16)	0.82 (0.18)
ACTIVE VISUAL HEAD IMPULSE TESTS		
Horizontal	0.91 (0.14)	0.93 (0.10)
Vertical	0.72 (0.08)	0.75 (0.10)
ACTIVE AUDITORY HEAD IMPULSE TESTS		
Horizontal	0.83 (0.13)	0.85 (0.14)
Vertical	0.65 (0.09)	0.71 (0.13)

Fig. 1 *Overview of VOR mean gain values (*ratio of eye- and head velocities) *and standard deviations (SD) for each of the individual tests presented for both session 1 and 2.*

CONCLUSIONS

The proposed method shows high face validity and excellent to good reliability for passive head impulse testing. However, further development is needed before this method can be used for active head impulse testing. Despite this, the described method is promising and could potentially have significant clinical implications in the future, where the system might help the clinician to distinguish between acute stroke and peripheral vestibular pathologies within the short available time after the onset of acute dizziness.

REFERENCES

1. Hülse R, et al. Peripheral Vestibular Disorders: An Epidemiologic Survey in 70 Million Individuals. Otol Neurotol. 2019;40: 88-95.
2. Huijbregts P, et al. Dizziness in Orthopaedic Physical Therapy Practice: Classification and Pathophysiology. Journal of Manual & Manipulative Therapy. 2013;12.
3. Singh NK, et al. Test-Retest Reliability of Video Head Impulse Test in Healthy Individuals and Individuals with Dizziness. J Am Acad Audiol. 2019;30: 744-752.
4. King WM. Getting ahead of oneself: Anticipation and the vestibulo-ocular reflex. Neuroscience. 2013;236: 210-219.
5. Koo TK, Li MY. A Guideline of Selecting and Reporting Intraclass Correlation Coefficients for Reliability Research. J Chiropr Med. 2016;15: 155-163.
6. Cognolato M, et al. Head-mounted eye gaze tracking devices: An overview of modern devices and recent advances. J Rehabil Assist Technol Eng. 2018;5: 2055668318773991.
7. Saredakis D, et al. Factors Associated With Virtual Reality Sickness in Head-Mounted Displays: A Systematic Review and Meta-Analysis. Front Hum Neurosci. 2020;14.

3D KINEMATIC MODELLING OF SHOULDER BIOMECHANICS

Stefan Jensen[1*], Catarina Malmberg[2], Kristoffer Barfod[2], Marie Traberg[1], and Jesper Bencke[3]

[1]Technical University of Denmark, [2]Department of Orthopaedic Surgery, Copenhagen University Hospital Hvidovre, [3]Human Movement Analysis Lab, Department of Orthopaedic Surgery, Copenhagen University Hospital Hvidovre

*Student

E-mail adresses: s184058@student.dtu.dk (Stefan Jensen), msene@dtu.dk (Marie Traberg), jesper.bencke@regionh.dk (Jesper Bencke), catarina.anna.evelina.malmberg.02@regionh.dk (Catarina Malmberg), kristoffer.barfod@regionh.dk (Kristoffer Barfod)

INTRODUCTION

Due to its unconstrained bony architecture, the glenohumeral joint is inherently one of the most unstable joints in the human body. The incidence of traumatic shoulder instability is 1.7%, of which more than 90% is in the anterior direction [1]. The possibility of investigating the glenohumeral displacement during dynamic tasks with the present diagnostic methods is limited. An alternative method based on optoelectronic motion analysis is proposed in this project. A known source of error associated with this method is soft tissue artefacts, defined as skin movement relative to the underlying bone. However, mathematical optimization procedures can be used to reduce the impact of this error [2].

The objective of this project was to measure the displacement of the humeral head relative to the glenoid cavity during dynamic tasks using an optoelectronic motion capture system and assess the feasibility of using the method in a clinical setting.

METHODS

A voluntary male aged 24 without clinical shoulder instability performed seven repeated movements of 0-90° abduction followed by maximal external rotation of the dominant shoulder joint. Only the five midmost repetitions were included due to potential errors associated with initializing and terminating the movement. Retroreflective markers were attached to the skin on the scapula and the humerus. Kinematic data from the markers were collected simultaneously using a VICON™ motion capture system and processed in MATLAB® subsequently.

Two different methods for tracking the segments of the scapula and the humerus kinematics were compared:

- the *classical method,* where the motion of any given segment is described by a segment-embedded local coordinate system defined from three markers
- the *optimized method,* based on a least-squares optimization procedure with more than three markers to define the segment-embedded local coordinate system.

RESULTS AND DISCUSSION

A maximum posterior translation of 25 mm was found during the motion task when calculated with the optimized method. The corresponding maximal translation for the classical method was 20 mm (Figure 1). This seems to be an overestimation when compared to reference kinematics obtained from markers secured on intracortical pins [3]. Furthermore, the performed movement would expect to induce anterior translation, if any [1].

The results demonstrate that the kinematics are affected by task dependent soft tissue artefacts independent of the method used. The least-squares optimization procedures are optimal in a least-square sense under two conditions: the noise associated with the markers are isotropic (equal distribution in all directions) and homogeneous (equal magnitude for all markers) [4]. However, our results confirm previous studies that these conditions do not hold true when skin markers are used [5], as the optimized method does not improve the soft tissue artefact error remarkably.

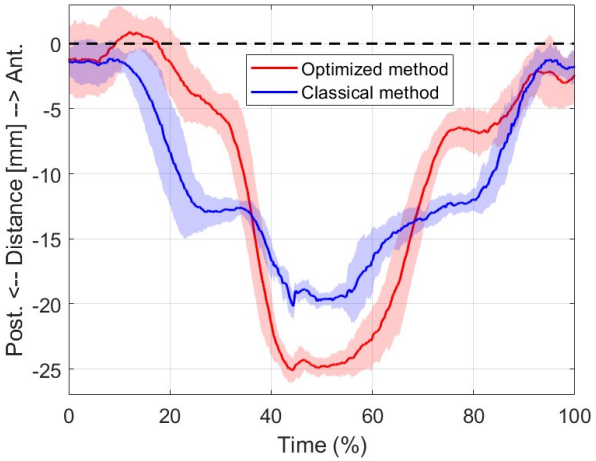

Fig. 1 The measured anterior-posterior glenohumeral displacement as a function of the time in % during the entire movement from and back to reference position. The graphs represent the mean displacement of the repetitions. The shaded area indicates the standard deviation.

CONCLUSIONS

Currently, none of the methods used in this project are sufficiently accurate to be used in a clinical context. Further investigation on algorithms that can correct for soft tissue artefacts is needed.

REFERENCES

1. Dumont GD, et al., *Current reviews in musculoskeletal medicine* **4**: 200-7, 2011
2. Monnet T, et al., "Improvement of the Input Data in Biomechanics: Kinematic and Body Segment Inertial Parameters". In: *Biomechanics: Principles, Trends and Applications*, 2010
3. Dal Maso F, et al., *Clinical Biomechanics* **29**: 1048-55, 2014
4. Halvorsen K, et al., *Journal of Biomechanical Engineering* **127.3**: 475-83, 2004
5. Blache Y, et al., *Journal of Biomechanics* **62**: 39-46, 2017

Does wearing a passive exoskeleton help during obstacle avoidance?

Cristina Pirscoveanu[1,*], J. Hansen[1], M. Pedersen[1], and P. Madeleine[1]
[1]Aalborg University, Department of Health Science and Technology, Aalborg, Denmark
*Ph.D. student civ@hst.aau.dk

INTRODUCTION

Exoskeletons were proven to assist during every day walking hazards or obstacles [1]. More specifically, the use of exoskeletons leads to increases in step length and gait velocity. Traditionally, most exoskeleton studies are carried out in laboratory settings [2], which is an inaccurate depiction of everyday outdoor conditions. Therefore, the aim of this study is to investigate the spatiotemporal gait parameters during outdoor challenging walking situations while wearing a passive hip exoskeleton.

METHODS

Twelve healthy male participants (25.4 ± 3.0 years, 183.8 ± 5.6 cm, 91.8 ± 13.3 kg) walked at their preferred speed on 3x10-meter outdoor courses with (EXO) and without a passive hip exoskeleton (noEXO). The exoskeleton used was aLQ, a bilateral passive assistive exoskeleton (IMASEN, Aichi, Japan). The participants had to walk normally with no obstacle (O1) and adjust their gait to the courses obstacles by stepping up unto a sidewalk (O2) and stepping over a pothole (O3). The obstacles had a height of 11 cm and a step over gap of 30 cm and were created artificially using similar materials as the walking surface. Five walking trials for each obstacle and exoskeleton conditions were collected. The order of the obstacles and exoskeletons were randomized. Each participant had a 10-minute familiarization period with the obstacles and the Xsens MTw Awinda. A sampling frequency of 100 Hz was used. Cadence, velocity, step length and double stance time were extracted. A one-way repeated measures (ANOVA) was conducted (p-value <0.05, inferred significance). The exoskeleton was used as within-subject variables for each of the parameters and obstacles. The effect size was extracted through Partial eta squared (η^2_p) where a value of 0.01, 0.06 and 0.14 was considered small, medium, and large, respectively.

RESULTS AND DISCUSSION

There was no significant effect of the exoskeleton for cadence (O1: F1,10=1.51, p=0.25, $\eta 2_p$=0.13; O2: F1,10=0.89, p=0.37, η^2_p=0.08; O3: F1,10=1.28, p=0.29, η^2_p=0.11), velocity (O1: F1,10=1.72, p=0.22, η^2_p=0.15; O2: F1,10=1.11, p=0.74, η^2_p=0.01; O3: F1,10=0.02, p=0.97, η^2_p=0.00), step length: (O1: F1,10=0.15, p=0.91, η^2_p=0.001; O2: F1,10=0.15, p=0.94, η^2_p=0.02; O3: F1,10=1.92, p=0.20, η^2_p=0.16) and double stance time (O1: F1,10=1.98, p=0.19, η^2_p=0.16; O2: F1,10=0.00, p=1.00, η^2_p=0.00; O3: F1,10=0.31, p=0.86, η^2_p=0.03).

Even though the results presented with no significant changes, the effect sizes were medium to large in some cases. Walking with no obstacle showed a large effect size for velocity and stance time (η^2_p>0.14**)**. Stepping up reported a medium effect size for cadence (η^2_p=0.08). Whereas stepping over had a medium effect size for cadence (η^2_p=0.11) and a large effect size for step length (η^2_p=0.16).

The results showed a 7% decrease in gait velocity when confronted with stepping over an obstacle, compared to the other obstacle conditions. Furthermore, a 20% decrease in double stance time was seen for stepping up compared with the other obstacles. Moreover, a 4% increase in cadence and a 1% decrease in double stance time was seen when wearing the exoskeleton and trying to step up onto an obstacle.

CONCLUSIONS

In conclusion, our findings indicated a small increase in cadence when wearing a passive hip exoskeleton for stepping up, but a small decrease for stepping over among young adults. Furthermore, the longer step lengths seem to be used when stepping up and walking with no obstacle compared to stepping over an obstacle. Whereas shorter double stance time was used when stepping up. These findings underlined the fact that gait was not significantly inhibited by wearing an exoskeleton during walking while navigating obstacles in young asymptomatic male adults. This could imply that the stability of gait is not hampered when walking and wearing a passive hip exoskeleton in outdoor challenging conditions in young adults.

ACKNOWLEDGEMENTS

We would like to thank IMASEN Electrical Industrial Co., Ltd, Aichi, Japan for allocating the required exoskeletons for this study.

REFERENCES

1. Zhang Z. et al. *Sensors* **20**(20): 5844, 2020
2. Muro-de-la-Herran A. et al. *Sensors* **14**(2):3362–94, 2014.

Table 1 Mean ± SD of spatiotemporal aspects for all obstacles, where O1 = no obstacle, O2 = step up, O3 = step over, EXO = wearing exoskeleton and noEXO = without wearing exoskeleton.

Condition	Cadence (steps/s)	Velocity (m/s)	Step Length (m)	Double Stance Time (ms)
O1. EXO	2.20 ± 0.17	1.37 ± 0.03	0.73 ± 0.04	83.23 ± 3.78
noEXO	2.08 ± 0.18	1.36 ± 0.03	0.73 ± 0.05	85.45 ± 5.87
O2. EXO	2.17 ± 0.15	1.39 ± 0.04	0.74 ± 0.08	66.06 ± 10.36
noEXO	2.09 ± 0.22	1.38 ± 0.04	0.74± 0.06	65.25 ± 7.75
O3. EXO	1.82 ± 0.17	1.28 ± 0.03	0.72 ± 0.09	82.85 ± 7.13
noEXO	1.93 ± 0.18	1.28 ± 0.05	0.75 ± 0.04	82.83 ± 7.85

FREELY CHOSEN CADENCE IS DEPENDENT ON PEDALLING HISTORY DURING ERGOMETER CYCLING

E. A. Hansen

Sport Sciences – Performance and Technology, Department of Health Science and Technology, Aalborg University, Denmark

INTRODUCTION

History dependence can refer to the fact that parts of the human (e.g. one or a group of muscles [1]), the nervous system [2, 3], or functional aspects of the human (e.g. stereotyped rhythmic motor behaviour [4], or performance [5]) depend on prior muscle activation. In the present study, it was investigated whether initial cycling at relatively low and high preset target cadences affected the subsequent freely chosen cadence at the end of the same bout of submaximal ergometer cycling. The cadence that occurs during cycling has a practical significance. As an example, the cadence can affect the result of a submaximal ergometer cycling test performed to evaluate training status.

METHODS

Healthy and recreationally active participants (18 males and 4 females, 185.0±9.8 cm, 79.9±10.0 kg, 23±2 years) performed one test session, which consisted of three bouts of submaximal (100 W) ergometer cycling. In one bout (A), cycling at 50 rpm was followed by cycling at freely chosen cadence. In another bout (B), cycling at 90 rpm was followed by cycling at freely chosen cadence. In yet another bout (C, considered a reference bout), the cadence was freely chosen throughout. Bouts were separated by 5 min rest. Behavioural (cadence), biomechanical (internal power [6] and pedal force profile characteristics), and physiological (heart rate) responses were determined.

RESULTS

Increased cadence generally resulted in increased internal power and decreased maximal tangential pedal force (F_{max}), and *vice versa*, in accordance with existing knowledge [7]. Initial cycling at 50 and 90 rpm caused freely chosen cadence to be, on average, around 5% lower and higher ($p < .05$), respectively, than the reference freely chosen cadence (see table and figure) at the end of the submaximal bout where the cadence was freely chosen. These differences in cadence were not accompanied by statistically significant differences in heart rate.

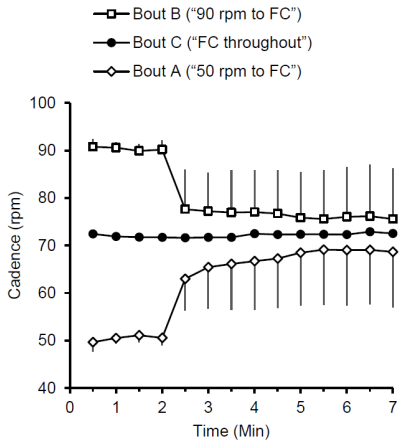

Cadence as a function of time during the three cycling bouts. There was a preset target cadence for the initial 2 min of bout A and B

DISCUSSION AND CONCLUSION

It is suggested that the freely chosen cadence is generated by an interplay between spinal neural networks, supraspinal input, and sensory feedback. Further, that the observed history dependence of the freely chosen cadence might be a result of neural inhibition and excitation, caused by neurotransmitter substances. In conclusion, the freely chosen cadence at the end of an ergometer cycling bout depended on the preset target cadence applied at the beginning of the bout. This finding may be denoted a phenomenon of motor behavioural history dependence.

REFERENCES

[1] Abbott BC & Aubert XM (1952) J Physiol 117:77-86
[2] Majczynski H *et al*. (2020) Front Neural Circuits 14:14
[3] Miller MW (2019) Biol Bull 236:144-56
[4] Hansen EA *et al.* (2015) J Mot Behav 47:490-96
[5] Young WB *et al*. (1998) J Strength Cond Res 12:82-84
[6] Minetti AE *et al*. (2004) Proc R Soc Lond B 268(1474):1351-60
[7] Hansen EA (2015) Acta Physiol 214(Suppl 702):1-18

	F_{max} (N)	Crank angle at F_{max} (°)	F_{min} (N)	Crank angle at F_{min} (°)	Internal power (W)
Bout A ("50 rpm to FC")					
Initially (at 50 rpm)	280±31	108±6	-66±23	311±10	7±1
Finally (at 68.6±11.1[a] rpm)	272±32[c]	109±6	-67±17	299±11	20±9[e]
Bout B ("90 rpm to FC")					
Initially (at 90 rpm)	232±24	107±11	-68±16	294±7	41±5
Finally (at 76.0±10.1[b] rpm)	261±27[d]	108±5	-68±16	298±10	26±11[f]
Bout C ("FC throughout")					
Finally (at 72.4±11.3 rpm)	265±29	110±6	-67±17	300±15	23±11

FC, freely chosen cadence. [a] and [b]Different from the cadence in bout C ($p < .05$). [c] and [d] Not different from bout C ($p > .05$). [e] and [f] Different from bout C ($p < .05$). F_{max}, maximal tangential pedal force. F_{min}, minimal tangential pedal force. $n = 22$. Data are mean ± SD (also in the figure)

ACKNOWLEDGEMENTS

Participants as well as the following AAU students who performed the data collection for a semester project: MH Andersen, A Andresen, M Johansen, SB Klausen, MG Lassen, R Lindegren, MD Nielsen, MØ Nielsen, FS Nielsen, E Nøddelund, MP Sørensen, MQ Thygesen

MEDIO-LATERAL AND LATERAL EDGE FRICTION IN INDOOR SPORTS SHOES

Timo Bagehorn[1], Filip Gertz Lysdal[1,2], Lasse Jakobsen[2], Mark de Zee[1], Uwe G. Kersting[1,3]

[1]Ph.D. student, Department of Health Science and Technology, Aalborg University, Aalborg, Denmark
[2]Department of Mechanical Engineering, Technical University of Denmark, Kgs. Lyngby, Denmark
[3]Institute of Biomechanics and Orthopaedics, German Sport University Cologne, Cologne, Germany

INTRODUCTION

It has previously been speculated that the occurrence and severity of lateral ankle sprain injuries is linked to excessive shoe-surface friction [1], [2]. Especially the lateral parts of the shoe outsole are suggested to play an important external role in this scenario, but have never been quantified in a systematic manner. Therefore, the purpose of this study was to investigate the variation of friction of indoor sport shoes with foot orientation and compare it to the traditional forefoot traction test.

METHODS

Twelve of the most popular indoor shoe models of the season 2017-18 were used for the mechanical friction tests. The test setup consisted of a steel frame that was bolted to the floor above a force plate-equipped mechanical hydraulic platform. All tests were conducted against a standard vinyl indoor sports floor (7.5 mm Taraflex – Evolution, Gerflor, FRA). Vertical and horizontal ground reaction forces were recorded using an AMTI force plate (Watertown MA, USA) which movements were captured via a single retro-reflective marker using eight infrared cameras (Qualisys AB, Gothenburg, Sweden). We conducted and modified ISO:13287:2019 [3] test for footwear slip resistance by positioning the shoe on its forefoot (7° pitch), lateral forefoot (7° pitch, 90° rotation) and lateral edge (15° pitch, 30° roll, 90° rotation) (Fig. 1). The latter two were supposed to replicate medio-lateral movements similar to previously reported ankle sprain incidents [4].

Tests were conducted with a constant normal force of 500N, translation distance of 120 mm and a sliding velocity of 0.3 m/s. Shoes were mounted to a last and fixed with their shoes laces. The friction coefficient for each shoe and test condition was then calculated for the time of horizontal plate movement via the horizontal and vertical reaction forces. The available dynamic friction coefficient (ACOF) was ultimately calculated as an average over the plateau following the peak in static friction, as per ISO: 13287:2019. A total of five repetitions was performed for each shoe and testing condition. For statistics, a two-way ANOVA was performed to analyze the effect of test type and shoe model on ACOF. Tukey's HSD post-hoc test was used to investigate differences between test setups and between shoe models. Additionally, a linear regression analysis was performed to test for correlations between testing conditions.

Fig. 1 Test setups, from left to right: anterior-posterior, medio-lateral, lateral edge. The arrow indicates the movement direction of the surface (hydraulic force plate).

RESULTS AND DISCUSSION

Simple main effects analysis showed that test type ($p<0.001$) and shoe model ($p<0.001$) both did have a statistically significant effect on ACOF. In general, we found that medio-lateral ACOF on average was 14% lower, and lateral edge friction 22% lower than anterior-posterior ACOF (Table 1). The test results demonstrate a large variability in ACOF between shoes and tests.

The linear regression analysis revealed that the ACOF of anterior-posterior significantly predicted medio-lateral and lateral edge ACOF ($y=0.55x+0.35$, $p=0.0008$ and $y=0.59x+0.21$, $p=0.002$). Here anterior-posterior accounted for 70% of the variation in medio-lateral ($R^2 = 0.7$, $p=0.0008$), and 63% of the variation in lateral edge ($R2 = 0.63$, $p=0.002$). However, these correlation coefficients are not strong, hence existing recommendations for anterior-posterior friction values can hardly be transferred to lateral movements.

In summary, this implies that if one wishes to accurately assess traction for other directions or areas, one should perform such specific tests accordingly.

Table 1 Mean ACOF by test setups. Significant difference compared to anterior-posterior (*) and to medio-lateral (~).

	Anterior-Posterior	**Medio-Lateral**	**Lateral Edge**
ACOF	1.18 ± 0.21	1.00* ± 0.14	0.91*/~ ± 0.16

CONCLUSIONS

This study showed that there is a significant difference in friction coefficient between a traditional forefoot test, the medio-lateral forefoot test and the modified lateral edge test. We suggest that if specific footwear friction properties need to be assessed accurately, then motion specific tests should be conducted. Future research needs to investigate if friction properties of different shoe outsole areas have clinical implications for injury prevention.

REFERENCES

1. Dragoo JL and Braun HJ, *Sport. Med.*, **vol. 40, no. 11**, pp. 981–990, Nov. 2010
2. Doherty C, et al., *Sport. Med.*, **vol. 44, no. 1**, pp. 123–140, 2014
3. ISO 13287:2019 - Personal protective equipment - Footwear - Test method for slip resistance, CEN
4. Fong DTP, et al., *J. Sport Heal. Sci.*, **vol. 00**, pp. 1–6, 2021

Bone tracking using A-mode ultrasound probes: evaluation of the initial guess

Ilias Theodorakos[1,*] and Michael Skipper Andersen[1]
[1]Department of Materials and Production, Aalborg University, Denmark

INTRODUCTION

Non-invasive measurements of bone movements have multiple potential applications within orthopedics and clinical gait analysis among others. To this end, the feasibility of using A-mode ultrasound-based technology was recently demonstrated [1]. The rationale behind using A-mode ultrasound probes is to measure the depth from the surface of the skin to a point on the bone and subquently compute the 3D coordinate of this point by tracking the probe in 3D space. Through simultaneous measurements of multiple A-mode probes, multiple 3D points on the surface of the bone can be obtained. These points are subsequently used to reconstruct the bone kinematics by employing Iterative Closest Point (ICP) algorithms, which minimize the distance between measured 3D points and the closest point on the surface of a 3D digitalized representation of the bone.

This reconstruction process has been shown to include multiple local minima and be sensitive to the initial guess for the applied optimizer [3]. Robust optimization algorithms are, therefore, desired to solve the ICP problem. In this study, we explored the so-called Complex optimization algorithm [4] and its sensitivity to the initial guess.

METHODS

A sheep femur cleaned from soft tissue was used in this study. The 'true' bone movement was tracked using a bone pin with attached markers. Moreover, the geometry of the bone and its attached markers was 3D scanned. Subsequently, the specimen was embedded into ballistic gel.

Measurements on four anatomical areas of the bone were obtained using a 7.5 MHz ultrasound A-mode probe (Figure 1). Four points per anatomical area and three repetitions per point were recorded. For each measurement, the probe was tracked with markers while it measured the distance from the surface of the ballistic gel to the bone surface.

The surface scans of the specimen, ultrasound measurements and the marker trajectories served as input to the ICP-based bone reconstruction algorithm that minimized the distance between the bone and the bone surface registration points in a least squared sense.

Subsequently, the bone registration errors were computed by comparing the results obtained from the ultrasound-based reconstruction of the bone and the bone pin markers based bone reconstruction.

Due to limitations in the available ultrasound hardware, we identified the sixteen measurements, four per anatomical area, that resulted in the smallest registration error. A sensitivity analysis was finally performed to evaluate the influence of the initial guess on the registration error. As the Complex algorithm randomly generates the starting population, which influences the registration error, each simulation was repeated 10 times.

Fig. 1 The probe and the specimen with the attached markers embedded into the ballistic gel.

RESULTS AND DISCUSSION

The sheep femur registration error was 0.34 (0.06) mm for the translation and 0.15 (0.12)° for the rotation. This is a positive outcome as it demonstrates accuracy comparable to medical imaging based registration procedures. Previously, a RMSE of 2.81 mm was reported for a human cadaveric femur registration using 25 registration points with a modified ICP method [2]. The differences in the results can be partially explained by the difference in the bone size and the fact that our specimen was embedded into ballistic gel that idealizes soft tissue acoustic properties.

The sensitivity analysis (Figure 2) revealed that the registration error is sensitive to perturbations around all axes. This outcome suggests that a good initial guess has to be provided in order to obtain accurate bone registration.

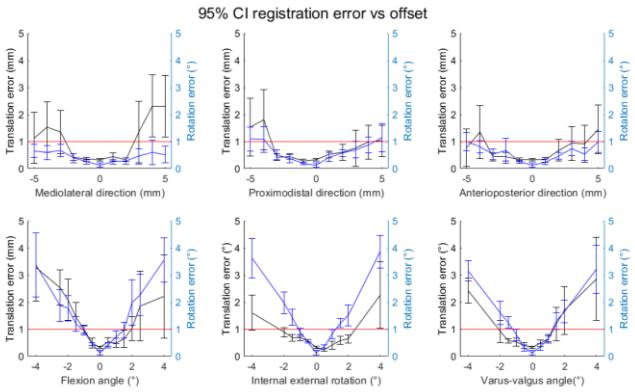

Fig. 2 95% confidence intervals of the translation and rotation registration error for the sheep femur specimen.

CONCLUSIONS

The presented results suggest that Complex optimization can be employed combined with the ICP to provide accurate registration of known bone geometry however, the registration error is sensitive to rotational perturbations of the initial guess. Procedures that ensure good initial guess should be implemented into the registration program.

REFERENCES

1. Niu K, et al., *CAOS*, pp. 166-170, 2017
2. Niu K, et al., *PLoS ONE*, **13(6)**: e0199136, 2018
3. Ma E and Ellis RE, *Med Image Anal*, **7:** 237-250, 2003
4. Box MJ, et al., *Computer J*, **8:** 42-52, 1965

The temporal pattern and the probability distribution of visual cueing can alter the structure of stride-to-stride variability

Peter C. Raffalt[1], Nick Stergiou[2,3], Joel H. Sommerfeld[2] and Aaron D. Likens[2]
[1] Department of Biology, University of Southern Denmark, Odense, Denmark
[2] Department of Biomechanics and Center for Research in Human Movement Variability, University of Nebraska at Omaha, Omaha, NE, USA
[3] College of Public Health, University of Nebraska Medical Center, Omaha, NE, USA.
Email: raffalt@biology.sdu.dk

Introduction

Sensorimotor synchronization during human locomotion is responsible for the entrainment of footsteps to the external cues from auditory and visual signals [1]. Additionally, the exposure to either auditory or visual pacing signals with different temporal patterns (e.g. pink or white noise) during walking has been reported to alter the temporal structure of the natural variability observed in the stride-to-stride time intervals [2]. However, it is unknown if differences in the temporal structure of stride-to-stride time intervals during paced walking originate from differences in the temporal pattern of the pacing signals or differences in the underlying probability distributions (e.g. normal or uniform distribution). The aim of the present study was to decipher the role of the temporal pattern and the probability distribution of the visual pacing cues on the temporal structure of the natural variability of the stride-to-stride time intervals during walking.

Methods

Ten healthy adults (male/female: 10/3; mean ± SD age: 25 ± 3.8 yrs; height: 1.77.2 ± 0.12 m; mass: 80.2 ± 16.1 kg) completed five overground walking trials with a minimum of 700 strides in each trial and 5 minutes of rest in-between. First, the participants completed self-paced walking (SPW). Then followed four trials in randomized order where visual cuing signals with different temporal pattern and probability distribution were provided through glasses with an in-build mini HDMI screen. The four signals were a) pink noise with a normal distribution (PNND), b) randomly shuffled pink noise with a normal distribution (SPNND), c) white noise with a normal distribution (WNND) and d) white noise with a uniform distribution (WNUD). The temporal structure of the stride-to-stride time intervals was quantified by the scaling exponent from the detrended fluctuation analysis where an exponent above 0.5 indicates statistical persistence, a scaling exponent below 0.5 indicates statistical anti-persistence and a scaling exponent equal to 0.5 indicate an uncorrelated random structure. A one-way Bayesian repeated measure ANOVA with post hoc between-trial comparisons was performed to investigate the effect of the different pacing signals on the scaling exponent.

Results and Discussion

There was decisive evidence to indicate that the type of pacing signal had an effect on the scaling exponent of the stride-to-stride time intervals (Bayers factor = 1.65 x 10^{10}, **Figure 1**, **Table 1**). The scaling exponents of the stride-to-stride time intervals during the SPW and PNND trial were close to 1 indicating statistical persistence. The scaling exponents during the SPNND, WNND and WNUD trials were close to 0.5 indicating uncorrelated random structure in the stride-to-stride time intervals. When altering the temporal pattern of the pacing signal from pink noise to shuffled pink noise or white noise, the temporal structure of the stride-to-stride time intervals became less statistical persistence and more uncorrelated. Similarly, when altering the probability distribution from normal to uniform the temporal structure of the stride-to-stride time intervals became even more uncorrelated and random. The results revealed that both the temporal pattern and the probability distribution of pacing signals influence the temporal structure of the stride-to-stride time intervals. Thus, the motor control of gait seems to prioritize not only the order in which sensory information is obtained but also a specific likelihood of informational input.

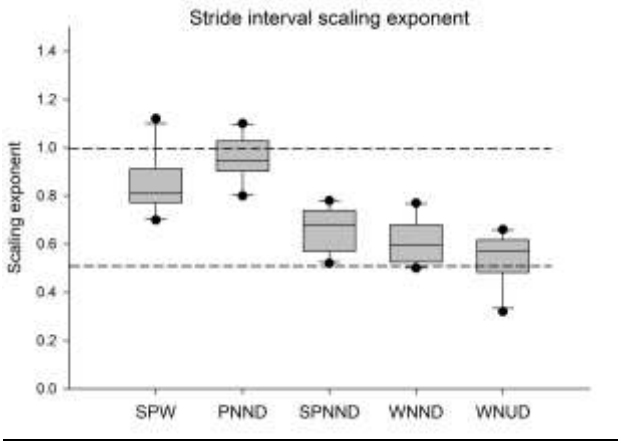

Figure 1: Scaling exponent of stride-to-stride time intervals.

Trial comparison		BF_{10}	Strength of evidence of trial difference
SPW	PNND	2.1	Weak or limited evidence
	SPNND	8.8	Substantial evidence
	WNND	15.7	Strong evidence
	WNUD	76.8	Very strong evidence
PNND	SPNND	555.1	Decisive evidence
	WNND	970.6	Decisive evidence
	WNUD	29775.7	Decisive evidence
SPNND	WNND	0.9	* Weak or limited evidence of no trial difference
	WNUD	9.8	Substantial evidence
WNND	WNUD	2.8	Weak or limited evidence

Table 1: Post hoc comparisons of scaling exponents from different trials. Bayers factor = BF_{10}.

References

[1] Sejdić E. et al. (2012). *PLoS One*, 7, e43104.
[2] Vaz JR. et al. (2020). *Front Physiol*, 11, 67.

A Modified Single Arm Machine- A Brief Report

Kent Klitgaard[1,2,*], Andreas Top Adler[2] and Mark de Zee[1]
[1] Sport Sciences, Department of Health Science and Technology, Aalborg University, 9220 Aalborg
[2]Team Danmark, 2605 Brøndby

INTRODUCTION

In strength training, it is essential to do sport-specific movements (1, 2). Several manufactures have developed a single arm stroke machine (SAM) to train or test the specific kayak stroke strength (3). However, the SAM has several issues: The frame is too short, athletes have pulled the sledge over the edge. The elastic bands could be tightened; however, this could add too much resistance as the sled will become too difficult to accelerate, affecting the movement of the stroke. Furthermore, the SAM does not accurately represent the fast stroke movements of sprint kayaking, as the inclination of the sled is too high. Lastly, athletes can pull the sled with a lesser specific kayak movement, which does not take the outwards motion of the blade in the water into account. In relation to the mentioned issues, it seems important to continue the development of the SAM to make it more specific and better to evaluate the maximal mechanical capacities of the muscles involved in a single stroke in kayaking.

The purpose of this study was to modify a SAM so the stroke movement would have a greater reassemble to the on-water kayak stroke.

METHODS

Design requirements

The SAM must be modified, so it ensures a proper kayak stroke is supported. The following requirements were therefore implemented:

- The paddler should be unable to pull upwards. The paddle must seek outwards as the wing blade does on the water
- A longer rail as the current is too short
- A lower inclination to ensure proper the proper force-velocity relationship
- Implementation of a force transducer to get force output from the SAM
- Implementation of a linear encoder to get velocity output from the SAM

Design

A SAM from the manufacture Dansprint Aps (Hvidovre, Denmark) was modified. The frame was elongated to 305cm, see figure 1 A1. A special frame (58 cm x 28 cm) was made to fit the sled see figure 1 C1.; on this frame, guiding rods were placed on each side of the sled see figure 1 A2. The rods have wheels on end to ensure minimal resistance from dragging the rods. The primary purpose of the rods was to ensure the stroke had an outgoing motion as on the water. The shaft was attached to the guiding rods with a sliding barrel joint see figure 1 B1. The shaft was connected metal wire going to the end of the frame to ensure maximal force transfer. A linear encoder (Chronojump Boscosystems, Barcelona, Spain) records the movement data of the SAM's sled. For this purpose, the recorder's cable was attached to the SAM's seat. The encoder was positioned on a support structure that kept it fixed and at an inclination of seven degrees to match the inclination of the sled's base. An S-beam force transducer was placed near the end of the wire that connects the shaft to the rail to get force measurements.

CONCLUSIONS

Research should be conducted on the modified SAM in to investigate how specific tests on the SAM relate to the athlete's performance on-water performance. Additionally, it should be investigated how the modified SAM compares to other conventional strength training exercises such as bench press and bench pull, which are shown to be essential for kayak sprint performance.

References

1. Issurin V. Training Transfer: Scientific Background and Insights for Practical Application. Sports Med. 2013 Aug;43(8):675-94.
2. Morin J, Samozino P. Interpreting Power-Force-Velocity Profiles for Individualized and Specific Training. International journal of sports physiology and performance. 2016 Mar;11(2):267-72.
3. Petrovic MR, García-Ramos A, Janicijevic DN, Pérez-Castilla A, Knezevic OM, Mirkov DM. The Novel Single-Stroke Kayak Test: Can It Discriminate Between 200-m and Longer-Distance (500- and 1000-m) Specialists in Canoe Sprint? International journal of sports physiology and performance. 2020 Sep 17,;16(2):208-15.

Figure 1: Overview of the modified SAM. A) a view of the sledge and guiding rods, B) a view of the shaft connection to the sledge and C) a views of the sledge from the other side

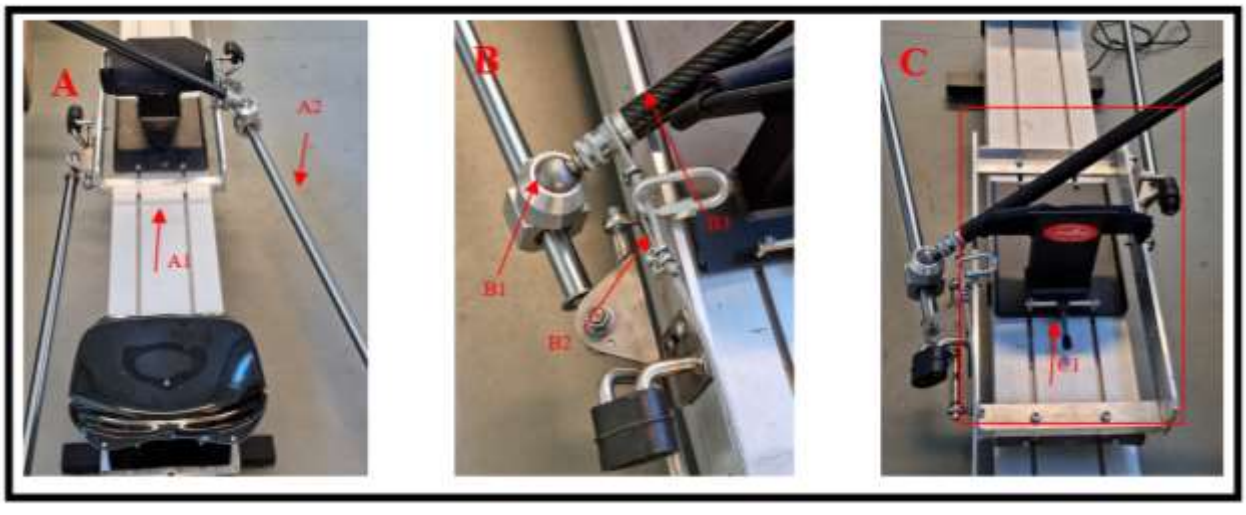

The apical vertebrae in mild scoliotic spines are subject to extremum weight moments

Mohammad Amin Shayestehpour[1*], Hamed Shayestehpour[2], Christian Wong[3], and John Rasmussen[2]
[1]Department of Mechanical Engineering, Sharif University of Technology, Tehran, Iran
[2]Department of Materials and Production, Aalborg University, Aalborg East, Denmark
[3]Department of Orthopedics, University Hospital of Hvidovre, Hvidovre, Denmark
Email: mohammadaminshayestehpour77@gmail.com

Introduction

Adolescent Idiopathic Scoliosis (AIS) is a three-dimensional deformity of the spine. The aetiopathogenesis for AIS is multifactorial and undetermined [1]. The weight of the upperbody segments on the spine can generate lateral bending moments which can potentially exacerbate the deformity during growth [2]. Keenan et al. (2015) showed that the lateral bending moment is maximum at the apical vertebra of Lenke1 scoliosis patients which was expected [2].

Methods

We utilized a recently developed and validated thoracolumbar musculoskeletal model in AnyBody modelling system [3,4] to simulate 13 patient-specific mild AIS cases [5] (average cobb angle = 16), which included 6 lumbar, 5 thoracic, and 2 thoracolumbar major curves. The AIS spines comprise 13 major and 8 minor curve apexes. The apex of a scoliotic spine is the vertebra with the farthest deviation from the midline of the vertebral column.

The weight moment (M_w) applied on each intervertebral joint was calculated in its horizontal cross-section (Figure 1. Left). The vertebral level with regional minimum and maximum of absolute values of M_w in the spine were selected and compared to the apical levels for each case.

Results and Discussion

Including all the major and minor curves, the weight moment on apexes was extremum in 95% of the cases.The regional maximum of M_w occurred at the apexes with the prevalence of 67%. The regional minimum happened in 28% of the cases in which the C7 vertebra had moved towards the major curve apex of a double curve spine. In scoliotic deformities, the center of mass deviates from the midline, and in order to maintain stability, C7 strays to either side of the midline. The translation of the C7 vertebra relative to the sacrum along the horizontal axis describes the coronal spinal balance. We speculated that C7 had laterally moved towards the major curve apex, which by definition is the most deviated vertebra, to reduce the high moment arm and consequently decrease the high values of M_w on the major curve apexes. C7 deviated towards the major curve apex in 85% of the cases. Speculating further, after the primary deformation is developed, the spine tends to reduce the unusual lateral bending moments by deviating C7 towards the primary curve apex. This potentially creates another convex and as the C7 gets closer to the major apex and further from the new minor apex, the weight moment increases on the minor apex, causing a vicious cycle.

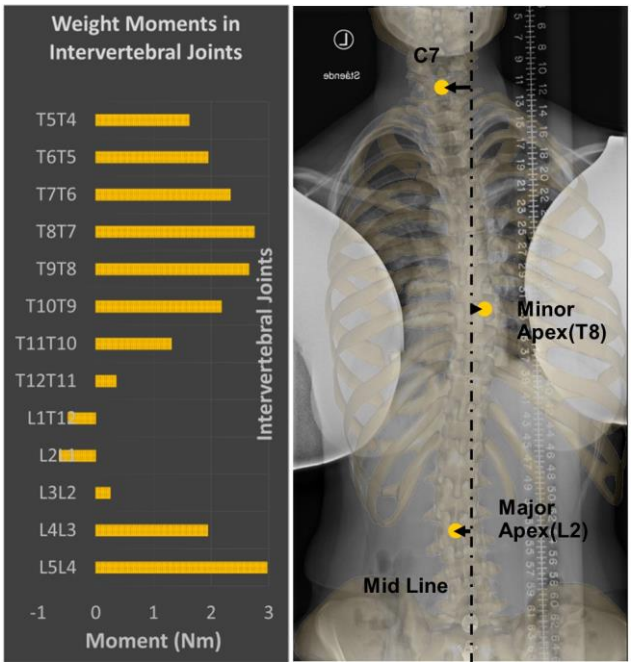

Figure 1: *Left:* The weight moment on intervertebral joints along the spine (N.m) for a patient. The moment is maximum at T8 (minor curve apex) and minimum at L2 (major curve apex). *Right:* Model projection on the radiograph of a patient. The C7 is laterally deviated towards the major curve apex and away from the minor curve apex.

Conclusion

Unexpectedly, we found that the weight moment on the apex of the AIS deformity was minimum in some of the cases, which happened due to the C7 lateral deviation towards the major curve apex. This finding indicates that the C7 moves in the same direction as the major curve apex in a compensatory reaction, and this can end up as a vicious cycle. Increasing the modeled cases and acquiring knowledge about their deformity progression allows further investigation of these speculations.

Acknowledgments

The project has received funding from the European Union's Horizon 2020 research and innovation programme under the Marie Sklodowska-Curie grant agreement NO. [764644].

References

[1] C. Wong, *Scoliosis*, **10**-1, 1–5, 2015
[2] B. Keenan, *Scoliosis* **10**-1, 1-11, 2015
[3] H. Shayestehpour, et al., *Multibody Syst. Dyn.*, 2021.
[4] H. Shayestehpour, et al., *Journal of Biomechanics*, Submitted
[5] H. Shayestehpour, et al., DBS 2021, Submitted

TREND VALIDATION OF METABOLIC MODELS AGSINST MEASUREMENTS USING INDIRECT CALORIMETRY

Nicki Lentz-Nielsen[1], Mads Daabeck Boysen[1], Mathias Munk-Hansen[1], Mike Steffensen[1,*], Andreas David Laursen[1],

Bjørn Keller Engelund[2], Kristoffer Iversen[2] & Mark de Zee[1]

[1]Department of Health Science and Technology, Sports Science – Performance and Technology, Aalborg University, Denmark
[2]AnBody Technology A/S, Aalborg, Denmark
*Student

INTRODUCTION

Muscuskeletal modeling can be used to estimate energy expenditure (EE). The AnyBody Modeling System (AMS) includes three litterature based methods of calculating EE: Margaria [1] uses a fixed efficiency of metabolic power to mechanical powerBhargava [2] and Umberger [3] focus on the relationsship between mechanical work and the associated heat production of the activated muscles.

These metabolic models do not appear to estimate EE for human walking accurately [4]. Where the prediction of EE in submaximal multiarticular tasks is even more challenging than maximal performing tasks, because the estimations should account for the muscle activations shared among the muscle synergists, antagonists as well as other related physiological responses [5]. Moreover, there exists less knowledge of the metabolic energetics of eccentric work [2,3]. Due to the inaccurate estimates of EE and the lacking knowledge of EE during concentric and eccentric contractions, the purpose of this study was to trend validate the three metabolic models in a concentric knee extension and eccentrick knee flexion at different loads using AMS.

METHODS

Five resistance trained adult males participated in the study. The overall study design consisted of three separate sessions. First session was to familiarize the subject with the concentric and eccentric contractions during a seated isokinetic knee-extension/flexion in the isokinetic dynamometer while wearing Pulmonary Gas Exchange (PGE) equipment. In the other two sessions the subject performed either concentric or eccentric contractions, in randomized order. 48h separated each session. A total of 150 contractions were performed for each contraction type and for each of the four loads: 20,40,60,80 Nm.

EE from the PGE system was calculated using Weir's formula [6]. An average repetition was calculated to represent all the 150 repetitions for each trial.

This average repetition was modelled in AMS to estimate EE.

RESULTS AND DISCUSSION

Figure 1 shows the agreement graphs between calculated and measured metabolic load. None of the models had a good agreement. Eccentric contractions performed worse than concentric. Furthermore, the linear regression of the experimental data, showed an R^2-value of 0.79 and 0.45 for concentric and eccentric contractions respectively. This indicates a large variance in metabolic power during eccentric contractions. This can be explained by eccentric contractions having a lower level of peripheral action potentials which can reduce the motor control of the movement [7]. The results for the concentric and eccentric contractions showed an overall underestimation of the metabolic output ranging from 25% to 100% by the three metabolic models compared to PGE. The tendency for underestimation increases with intensity level as seen in Figure 1. The underestimation from Bhargava [2] and Umberger [3] could be caused by the fact that their models are developed by using frog and mammalian muscles respectively, since the energetics of muscles from different species are different. The underestimation of Margaria [1] can be caused by the fixed coefficients of EE determined solely by the type of contraction during walking. Therefore, it does not consider the hyperbolically increasing oxygen demand by the respiratory system and other related physiological responses [8].

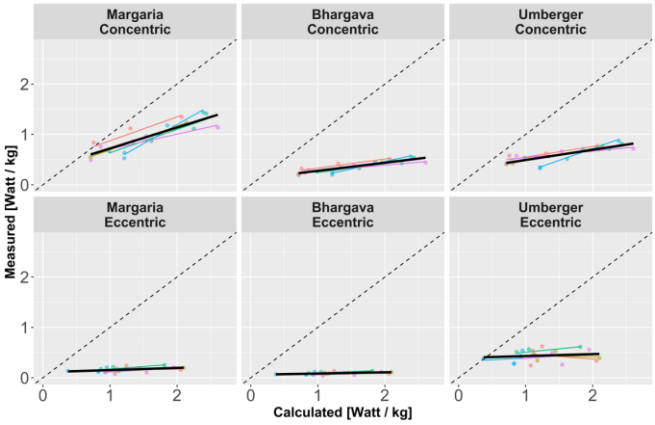

Fig. 1 Agreement between calculated (x-axis) and measured (y-axis) metabolic power. Dashed line indicates perfect agreement. Colored lines represent individual subjects, and the black line is the mean of all subjects.

CONCLUSIONS

Based on the presented results, the three metabolic models do not appear to be valid for isokinetic concentric and eccentric contractions of the m. quadriceps using computer based musculoskeletal models, compared to the experimental measurements of indirect calorimetry.

REFERENCES

1. Margaria, R. J *Internationale Zeitschrift für angewandte Physiologie einschliesslich Arbeitsphysiologie* **25**: 339-351, 1968
2. Bhargava L, et al., *J of Biomechanics* **37**: 81-88, 2004
3. Umberger, B, et al., *Computer Methods in Biomechanics and Biomedical Engineering*, **6**: 99-111, 2010
4. Koelewijn, A.D, et al., *PLOS ONE* **14**, 2019
5. Tsianos, G.A, & Macfadden, L. N, *PLoS Computational Biology* **12**, 2016
6. Weir, J. B. d. V, *J of Phys* **109:** 1-9, 1949
7. Enoka, R. M, *J of Applied Phys* **81**: 2339-2346, 1996
8. Otis, A.B, *Handbook of Physiology*, 463-476, 1964

THE EFFECT OF MASS DISTRIBUTION OF A LOWER BODY PASSIVE EXOSKELETON ON JOINT MOMENTS

Cristina Pirscoveanu[1,*], E. A. Hansen[1], J. Franch[1], and P. Madeleine[1]

[1]Aalborg University, Department of Health Science and Technology, Aalborg, Denmark, *Ph.D. student civ@hst.aau.dk

INTRODUCTION

Exoskeletons (EXO) have proven to assist humans during every day walking and prevent falling or tripping [1]. Many leg EXOs are comprised of interconnected mechanical parts attached to the lower body segments [2]. The mass of this mechanical construction commonly varies from 4.2 kg to 35.0 kg, depending on structure and actuation used [3]. aLQ (IMASEN, Aichi, Japan) is a light weight lower body passive EXO with a mass of .90 kg, designed to aid hip flexion. However, whether the mass distribution between this EXO's mechanical segments, influences the joint moments, is unclear. The purpose of this study was to determine which mass distribution should be used for further studies involving aLQ.

METHODS

In an exploratory pilot study, eight healthy participants (28.1±2.8 years, 180.0±0.08 cm, 85.4±24.4 kg) walked at their preferred speed on a 10-meter laboratory track with (EXO) and without the EXO (noEXO) for 5 trials in each EXO condition in one experimental protocol. Lower extremity gait kinematics and ground reaction forces were recorded and 10 steps/participant/condition were analyzed using Visual3D software. A lower limb 3D-model was created. The EXO was modeled bilaterally with two segments (Exo1 & Exo2), attached to the hip and thigh using a 1 degree-of-freedom (DOF) joint. Between the two EXO segments, a 3-DOF joint was created. Within Visual3D, three simulations were conducted (**S1:** .45 kg for Exo1 & 0 kg for Exo2; **S2:** .35 kg for Exo1 & .10 kg for Exo2 – actual mass of EXO, **S3**: 0 kg for Exo1 & .45 kg for Exo2) where the mass of the EXO segments varied with the assumption that the laboratory kinematics wouldn't be influenced by the mass distribution as long as the overall mass is constant. The 3-DOF joint moments were extracted for the EXO, hip, knee, and ankle for all 3 simulations using Visual3D inverse dynamics. The mean value of the normalized joint moment to 100% of the stance was used. The data from both the left and right leg were used. One-way repeated measures ANOVA and a post-hoc with Bonferroni correction were conducted ($p<.05$ inferred significance). The mass distribution simulations and NoEXO conditions were used as within-subject variables for each of the parameters.

RESULTS AND DISCUSSION

There was no significant effect of mass distribution on all joint moments in all directions ($p>.05$). No significant differences were found for the EXO moment ($p>.05$). However, the hip joint moment was significantly decreased by around 24% for EXO compared to NoEXO during flexion/extension (X) and increased by around 13% during abduction/adduction (Y) ($p<.05$, Table 1) for all three simulations. The knee and ankle moments were unaffected by the EXO's mass distribution simulations ($p>.05$).

CONCLUSIONS

The alterations of joint moments induced by the change in the EXO's mass distribution were small, below 1%, indicating that the EXO's mass distribution does not probably affect normal walking. Therefore, further studies investigating aLQ will model the EXO using the second simulation mass values. Interestingly, the hip moment was significantly reduced during flexion/extension when wearing the EXO underlining that light EXOs used by healthy participants aid during flexion/extension and increase the abduction/adduction hip moment.

ACKNOWLEDGEMENTS

IMASEN Electrical Industrial Co., Ltd, Aichi, Japan allocated the exoskeletons for this study.

REFERENCES

1. Panizzolo F et al. *Assistive Technology* **11:** 1–6, 2021
2. Jin X et al. *ICRA* 1772–77, 2017
3. Sanchez-Villamañan M et al. J *Neuroeng Rehabil* **16**(1): 55, 2019

Table 1 Mean ± SD joint moment for the exoskeleton (**EXO**), hip, knee, and ankle in **X** (flexion/extension), **Y** (abduction/adduction) and **Z (**internal/external rotation). * Statistically different from S1, S2 and S3 ($p<.05$)

		S1	S2	S3	NoEXO
EXO	**X**	0.001 ± 0.003	0.001 ± 0.002	0.000 ± 0.000	-
(Nm/kg body mass)	**Y**	0.002 ± 0.002	0.001 ± 0.001	0.000 ± 0.000	-
	Z	0.004 ± 0.002	0.003 ± 0.002	0.000 ± 0.000	-
Hip	**X**	0.138 ± 0.456	0.148 ± 0.459	0.148 ± 0.459	**0.187 ± 0.467** *
(Nm/kg body mass)	**Y**	0.528 ± 0.330	0.524 ± 0.331	0.524 ± 0.331	**0.464 ± 0.326 ***
	Z	0.142 ± 0.110	0.141 ± 0.109	0.141 ± 0.109	0.098 ± 0.095
Knee	**X**	0.118 ± 0.236	0.121 ± 0.238	0.120 ± 0.237	0.112 ± 0.254
(Nm/kg body mass**)**	**Y**	0.178 ± 0.123	0.178 ± 0.123	0.178 ± 0.123	0.184 ± 0.132
	Z	0.015 ± 0.078	0.015 ± 0.078	0.014 ± 0.078	0.017 ± 0.073
Ankle	**X**	0.075 ± 0.092	0.075 ± 0.091	0.075 ± 0.091	0.076 ± 0.090
(Nm/kg body mass)	**Y**	0.123 ± 0.155	0.123 ± 0.156	0.123 ± 0.156	0.122 ± 0.146
	Z	0.054 ± 0.062	0.054 ± 0.061	0.054 ± 0.061	0.051 ± 0.058

THE EFFECT OF CUTTING TASK COMPLEXITY ON TECHNIQUE VARIABLES ASSOCIATED WITH INCREASED RISK OF ACL INJURIES IN FEMALE HANDBALL PLAYERS

Kevin Bill[1, *], Patrick Mai[1], Mireia Claramunt Molet[2, 3], Julia Bartsch[4], Mathias Eggerud[5], Anniken Pedersen[6], Reidar Berg Moss[6], Katharina Glöckler[1], Fredrik Sæland[5], Steffen Willwacher[7], Uwe Kersting[1], Ola Eriksrud[6] and Tron Krosshaug[5]
[1]Institute of Biomechanics and Orthopaedics, German Sport University Cologne, [2]Digital Health Unit, Eurecat Centre Tecnològic de Catalunya, [3]Biomechanical Engineering Lab, Universitat Politècnica de Catalunya, [4]University of Konstanz, [5]Sports Medicine, Norwegian School of Sport Sciences, [6]Physical Performance, Norwegian School of Sport Sciences, [7]Mechanical and Process Engineering, Offenburg University
*Ph.D. student; email: k.bill@dshs-koeln.de

INTRODUCTION

The majority of anterior cruciate ligament (ACL) injuries in team sports are non-contact injuries, with cutting maneuvers identified as high-risk tasks [1]. Young female handball players have been shown to be at greater risk for ACL injuries than males [2]. One risk factor for ACL injuries is the magnitude of the knee abduction moment (KAM) [3]. Cutting technique variables on foot placement, overall approach and knee kinematics have been shown to influence the KAM [4]. Since injury risk is believed to increase with increasing task complexity, the purpose of the study was to test the effect of task complexity on technique variables that influence the KAM in female handball players during fake-and-cut tasks.

METHODS

Full-body kinematics of 51 female handball players (mean ± SD: 66.9 ± 7.8 kg, 1.74 ± 0.06 m, 19.2 ± 3.4 years) were captured using a 24-camera motion capture system (Qualisys AB, 200 Hz) and force plates (AMTI, 1000 Hz). Subjects were instructed to perform full-effort fake-and-cut tasks of three different complexities at a randomized order. For Task 1 (T1), subjects performed a pre-planned fake and cut without a defender or handling a ball. For Task 2 (T2), subjects caught a pass before performing a pre-planned fake and cut in front of a static defender. For Task 3 (T3), a defender was added to either side of the static defender of T2. At the instance of the catch, the middle defender and one of the additional defenders (randomized) moved toward the subject, resulting in an unanticipated cut direction. Cutting leg for T1 and T2 was determined based on player position, and T1 and T2 were performed on that leg only. Raw marker trajectories and force plate data were filtered with a cut-off frequency of 20 Hz and used to calculate full-body biomechanics [5]. Data of the leg determined for T1 and T2 of at least five valid trials were averaged for all tasks. Most significant predictors for KAM [4] were calculated (see Table 1). Differences in technique variables between tasks were calculated using a repeated-measures ANOVA (α = .05). Post-hoc analysis was performed using Bonferroni-corrected alpha levels, and the effect size was calculated using partial eta squared (η_p^2).

RESULTS AND DISCUSSION

The repeated measures ANOVA showed a statistically significant main effect of task complexity on foot-floor angle (p = .043), cut angle (p < .001), cut width (p < .001) and approach speed (p < .001). Measurement and post-hoc analysis results are shown in Table 1. Center of mass (CoM) trajectories of the cuts are shown in Figure 1.

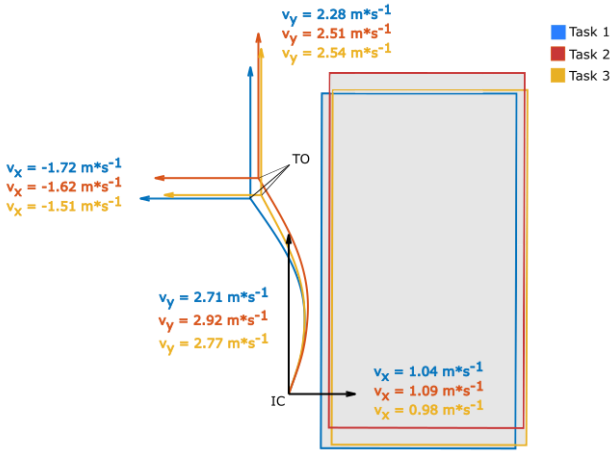

Fig. 1 CoM trajectories (N = 765) and horizontal velocities at initial contact (IC) and toe-off (TO) for the three tasks relative to the force plate (gray). Data of left-foot cuts (n = 75) were mirrored vertically. The location of the CoM at IC was used as the reference position.

CONCLUSIONS

Of the cutting technique variables that affect the KAM the most [4], only those related to the CoM are significantly affected by varying the task complexity. If foot placement and knee kinematics are only marginally affected, a selection of a few tasks might be sufficient to screen athletes.

REFERENCES

1. Krosshaug T, et al., *Am J Sports Med*, **32**: 359-367, 2007
2. Renstrom P, et al., *Br J Sports Med*, **42**: 394-412, 2008
3. Myer GD, et al., *Br J Sports Med*, **49 (2)**: 118-122, 2015
4. Kristianslund E, et al., *Br J Sports Med*, **48**: 779-783, 2014
5. Willwacher S, et al., *Footwear Sci*, **8**: 99-108, 20

Table 1 Results for the technique variables across the three tasks.

	Task 1	Task 2	Task 3
Knee valgus at IC (°), η_p^2 = .044	-6.26 ± 3.76	-5.79 ± 3.44	-6.46 ± 3.57
Foot-floor angle* at IC (°)†, η_p^2 = .061	14.26 ± 9.76	16.50 ± 10.59	13.93 ± 9.84
Cut angle (°)‡, η_p^2 = .270	70.51 ± 14.14^{C3‡}	69.54 ± 14.78^{C3‡}	61.52 ± 14.00$^{C1\ddagger, C2\ddagger}$
Cut width (°)‡, η_p^2 = .194	21.12 ± 2.52^{C3‡}	21.42 ± 2.76^{C3†}	22.79 ± 3.05$^{C1\ddagger, C2\dagger}$
Approach speed (m*s^{-1})‡, η_p^2 = .234	3.75 ± 0.47^{C2†}	4.01 ± 0.48$^{C1\dagger, C3\dagger}$	3.77 ± 0.48^{C2†}

*****angle between long axis of the foot and its projection on the floor (positive values indicate toe landing)
$^{\dagger}p$ < .05; $^{\ddagger}p$ < .001